Active Position and Vibration Control of a Flexible Links Mechanism Using Model-Based Predictive Control

Paolo Boscariol
e-mail: paolo.boscariol@uniud.it

Alessandro Gasparetto
e-mail: gasparetto@uniud.it

Vanni Zanotto[1]
e-mail: vanni.zanotto@uniud.it

Department of Electrical, Managerial, and Mechanical Engineering,
University of Udine,
Via delle Scienze 208,
33100 Udine, Italy

In order to develop an efficient and fast position control for robotic manipulators, vibration phenomena have to be taken into account. Vibrations are mainly caused by the flexibility of manipulator linkages, especially when dealing with high-speed and lightweight robots. In this paper, a constrained model-based predictive control is employed for controlling both position and vibrations in a mechanism with high link flexibility. This kind of controller has so far been used mainly to control slow processes, but here simulation results that show its effectiveness in dealing with high-speed and nonlinear processes are presented. The mechanism chosen to evaluate the performances is a four-link closed chain mechanism laying on the horizontal plane and driven by a single torque-controlled electric motor. [DOI: 10.1115/1.4000658]

1 Introduction

In the past 40 years modeling, dynamics, and control of flexible links mechanisms have been a central topic in robotics. The fact that accurate dynamic and control of vibration phenomena would allow to design and build robots with reduced weight and higher operative speed has been the main reason of this popularity. Accurate modeling of both single and multibody flexible links mechanism have been studied in a great deal of works. An extensive review of the results obtained so far can be found in Ref. [1]. Among the different approaches to dynamics modeling, the finite-element method (FEM) is the most popular. This approach, which is based on the discretization of elastic deformation into a finite set of nodal displacements, has been used, for example, in Refs. [2,3].

The aim of this paper is to investigate the effectiveness of model-based predictive control (MPC) strategy for position and vibration control in a multilink flexible mechanism, following the results already developed by the same authors in Ref. [4]. MPC refers to a family of control algorithms that compute an optimal control sequence based on the knowledge of the plant and on the feedback information. These data, together with a set of constraints, are used as the basis of an optimization problem. MPC control has been first employed in chemical factories, but in recent years it has experienced a wider diffusion to other industrial fields. The availability of more powerful embedded platforms in recent years has encouraged the development of embedded MPC control systems suitable to fast-dynamic plants. In this paper the MPC control is proposed for simultaneous position and vibration control in a four-link flexible mechanism lying on the horizontal plane. The literature on MPC as an effective vibration reduction strategy in flexible systems is very limited. To the authors' knowledge the only paper focusing on this topic is Ref. [5], in which an MPC controller is used to control vibrations in a flexible rotating beam through an electric motor and piezoceramic actuators. In this paper the MPC controller has been implemented in a software simulation using MATLAB/SIMULINK®. Exhaustive simulations have been made to prove the accuracy and the effectiveness of this control approach.

2 Dynamic Model of a Four-Link Planar Mechanism

In this section the dynamic model of a flexible-link mechanism proposed by Giovagnoni [3] will be briefly explained. The choice of this formulation among the several proposed in the last 40 years has been motivated mainly by the high grade of accuracy provided by this model, which has been proved several times, for example, in Refs. [6,7]. The main characteristics of this model can be summarized in four points: (1) finite element method (FEM), (2) equivalent rigid-link system (ERLS), (3) mutual dependence of rigid and flexible motion, and (4) suitability to mechanisms with an arbitrary number of both flexible and rigid links.

Each flexible link belonging to the mechanism is divided into finite elements. The motion of the mechanism can be thought as the superposition of the motion of an equivalent rigid-link system (ERLS) and the elastic motion of the nodes of the finite elements. Therefore, the free coordinates of the system are the angular position q of the crank and the vector of the nodal displacements $\mathbf{u}$. The nonlinear dynamic equations of motions of the system are

$$\begin{bmatrix} \mathbf{M} & \mathbf{MS} & 0 & 0 \\ \mathbf{S}^T\mathbf{M} & \mathbf{S}^T\mathbf{MS} & 0 & 0 \\ 0 & 0 & \mathbf{I} & 0 \\ 0 & 0 & 0 & \mathbf{I} \end{bmatrix} \begin{bmatrix} \ddot{\mathbf{u}} \\ \ddot{\mathbf{q}} \\ \dot{\mathbf{u}} \\ \dot{\mathbf{q}} \end{bmatrix} = \begin{bmatrix} \mathbf{M} & \mathbf{I} \\ \mathbf{S}^T\mathbf{M} & \mathbf{S}^T \\ 0 & 0 \\ 0 & 0 \end{bmatrix} \begin{bmatrix} \mathbf{g} \\ \mathbf{f} \end{bmatrix} + \begin{bmatrix} -2\mathbf{M}_G - \alpha\mathbf{M} - \beta\mathbf{K} & -\mathbf{M}\dot{\mathbf{S}} & -\mathbf{K} & 0 \\ \mathbf{S}^T(-2\mathbf{M}_G - \alpha\mathbf{M}) & \mathbf{S}^T\mathbf{M}\dot{\mathbf{S}} & 0 & 0 \\ \mathbf{I} & 0 & 0 & 0 \\ 0 & \mathbf{I} & 0 & 0 \end{bmatrix} \begin{bmatrix} \dot{\mathbf{u}} \\ \dot{\mathbf{q}} \\ \mathbf{u} \\ \mathbf{q} \end{bmatrix} \tag{1}$$

in which $\mathbf{g}$ and $\mathbf{f}$ are the vector of gravity forces and the vector of the external forces, respectively. This dynamic model is nonlinear, due to the quadratic relation between the nodal accelerations and the velocities of the free coordinates (see Ref. [8]). Therefore, it cannot be used as a prediction model for a linear MPC controller. In order to develop a state-space form linearized version of the dynamic system, the linearization procedure developed by Gasparetto [9] has been used. From Eq. (1), the best choice for the state vector is $\mathbf{x}=[\dot{\mathbf{u}},\dot{\mathbf{q}},\mathbf{u},\mathbf{q}]^T$.

The mechanism that has been chosen as the basis of the simulations is made by three steel rods, whose mechanical properties are described in Table 1 (see Fig. 1). These three rods are connected on a closed-loop planar chain employing three revolute joints. The first and the third links (counting anticlockwise) are connected to a chassis (the fourth link), which can be considered perfectly rigid. The rotational motion of the first link can be imposed through a torque-controlled electric motor. The whole chain can swing along the horizontal plane, so the effects of gravity on both the rigid and elastic motions of the mechanism can be neglected.

The crank and the coupler have been modeled with a single finite element. For the follower, two finite elements have been used, since it is the longer one. Increasing the number of finite

[1]Corresponding author.

Contributed by the Dynamic Systems Division of ASME for publication in the JOURNAL OF DYNAMIC SYSTEMS, MEASUREMENT, AND CONTROL. Manuscript received September 17, 2008; final manuscript received September 18, 2009; published online December 22, 2009. Assoc. Editor: J. Karl Hedrick.

Table 1 Kinematic and dynamic characteristics of the flexible link mechanism

	Symbol	Value
Young's modulus	E	210×10^{9} Pa
Flexural inertia moment	J	11.102×10^{-10} m^4
Beam's width	a	6×10^{-3} m
Beam's thickness	b	6×10^{-3} m
Mass/unit of length of link	m	272×10^{-3} kg/m
Crank length	L_1	0.3728 m
Coupler length	L_2	0.525 m
Follower length	L_3	0.632 m
Ground length	L_4	0.3595 m
Rayleigh damping constants	α	8.72×10^{-2} s^{-1}
	β	2.1×10^{-5} s

elements will certainly improve the overall accuracy of the model; however, this also increases the computational effort required for the simulations. Each single finite-element link has six elastic degrees of freedom, whereas the two finite-element link has nine degrees of freedom. After putting together the three links on the frame, and neglecting one of the nodal displacements in order to make the system solvable (see Ref. [3]), the resulting flexible system is described by 12 nodal elastic displacements and one rigid degree of freedom. All the nodal displacements are chosen, as in Fig. 2.

The MPC controller that will be introduced in the following paragraphs requires for the whole state vector $\mathbf{x}$ to be available; however, in practical applications it is impossible to measure all 12 nodal displacements (and their time derivatives) belonging to the state vector. For this reason a Kalman observer has been employed. This allows to get an estimation of the whole state vector $\mathbf{x}$ from measurements of u_9, u_{10}, and q. The accuracy of such an observer is shown in Fig. 3, where a comparison of the actual and estimated values of nodal displacement u_{12} is shown as an example. The same likeness holds for all the other estimated elements of the state vector.

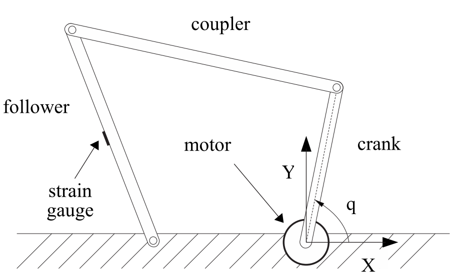

Fig. 1 The four-link mechanism used for simulations

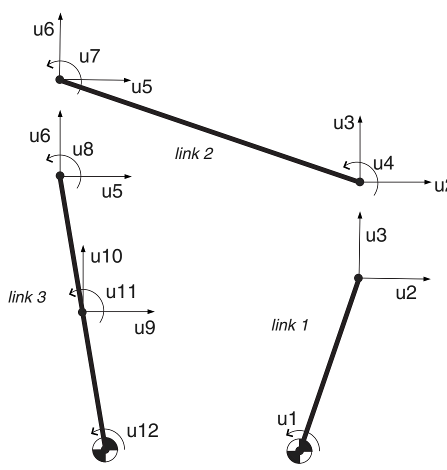

Fig. 2 Elastic displacements in the four-link mechanism

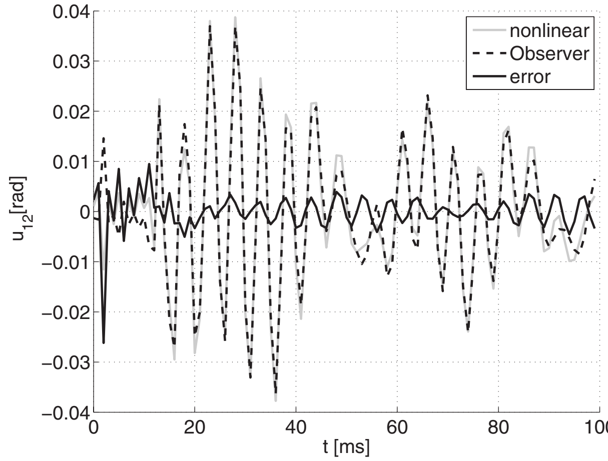

Fig. 3 Displacement vibration u_{12}: actual value, observed value, and error

3 MPC Control: Numerical Results

In this section a very brief explanation of the employed MPC controller will be presented. More details can be found in Ref. [10]. Basically, MPC control law is calculated as an optimization problem, whose evolution is influenced by both the plant actual inputs/outputs and its estimated future behavior, which is computed for H_p steps, H_p being the prediction horizon. The optimal control sequence $w(k)$, whose length is H_c (i.e., the prediction horizon) is calculated as the minimum of the cost function $\mathcal{V}(k)$

$$\mathcal{V}(k)=\sum_{i=1}^{H_p}\|\hat{\mathbf{z}}(k+i\times k)-\mathbf{r}(k+i)\|^2_{\mathbf{Q}(i)}+\sum_{i=0}^{H_c-1}\|\Delta\hat{w}(k+i\times k)\|^2_{\mathbf{R}(i)} \tag{2}$$

$\mathbf{Q}$ and $\mathbf{R}$ are diagonal matrices of weights, while $\hat{\mathbf{z}}(k)$, $\hat{w}(k)$, and $\mathbf{r}(k)$ are the vector of controlled variables, the control variable, and the reference trajectory, respectively. The weights that have been used in this work are: $\mu_9=0$, $\mu_{10}=1\times10^6$, and $\mu_q=1\times10^4$, which are the weights on nodal displacements u_9, u_{10}, and on angular position q, respectively. Moreover, this minimization problem is constrained, meaning that some limits can be imposed on control and controlled variables. Here these inequality constraints have been used

$$-2\times10^{-3}\le u_{10}\le 2\times10^{-3}\ \text{(m)}$$

$$\pi/36\le q\le \pi/4\ \text{(rad)}$$

$$-10\le w\le 10\ \text{(N m)}$$

w being the control variable, i.e., the torque provided by the actuator. There are other parameters whose values affect the behavior of the MPC controller. They are the prediction horizon H_p, the control horizon H_c, and the sampling period T_s. The effects of such parameters can be understood by looking at Figs. 4–10, where the results of the most meaningful simulations are shown. All the simulations have been conducted feeding the controller with a step reference for the angular position of the crank that moves from $\pi/36$ rad to $\pi/4$ rad (from 5 deg to 45 deg). Figure 4 shows the effects of the horizon control H_c, as far as the rigid rotation q is concerned. It can be seen that H_c affects both the response quickness and the steady state error.

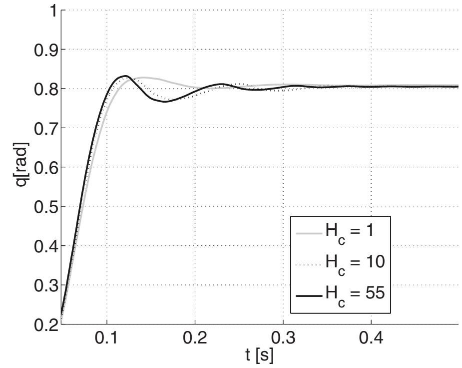

Fig. 4 Angular position of the crank q: H_c ranging from 1 to 55. H_p=35 and T_s=1 ms.

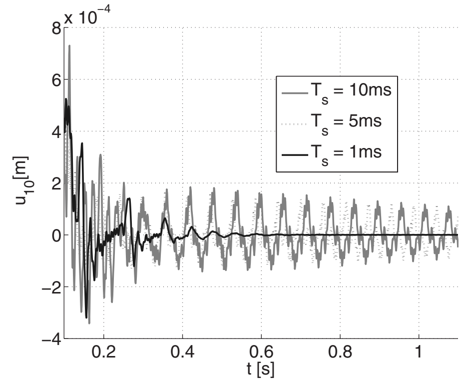

Fig. 7 Elastic displacement u_{10}: T_s ranging from 1 ms to 10 ms. H_p=35 and H_c=10.

At the same time a higher value of H_c improves also the vibration damping, as it is shown in Fig. 5. However, it must be recalled that the longer the horizon control length is, the bigger the computational controller requirements become [10]. Therefore, H_c should be chosen accordingly to the hardware capabilities and the requirements on the system behavior.

Figures 6 and 7 show the system performances when the sampling period changes from T_s=1 ms to T_s=10 ms. It is important to study the effects of the sampling period, proven that the higher the sampling period is, the lower the hardware computational requirements are, since the online control optimization must be repeated at each sampling instant. From the mentioned figures, it can be observed that the system behavior deteriorates as the sampling period increases. This performance can be imputed to the observer behavior, which becomes unable to estimate the real system state (Fig. 8) when the sampling interval increases.

In Figs. 9 and 10 the effects of the prediction horizon H_p are shown. In this case, the simulations have been carried out by supposing that mismatches between the real system and the modeled plant exist. In particular, the first link length has been underestimated of a 5%, as well as the masses of all the links have been underestimated by the same percentage. Moreover, a white noise has been added to the torque input, and the dynamic behavior of the electric actuator has been inserted in the system, modeled as a first order low-pass filter. Finally, a further mismatching between the commanded and the applied torque has been assumed. In particular, it is assumed that the voltage-torque gain of the real system has been 5% underestimated. The mentioned figures show that the system robustness can be improved by increasing the

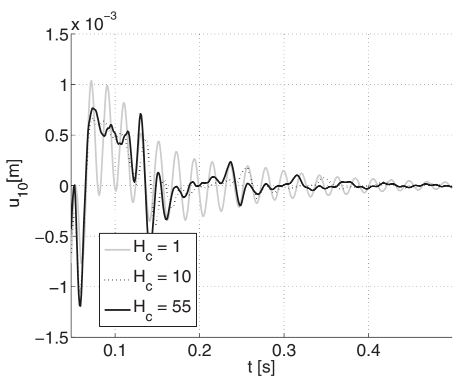

Fig. 5 Elastic displacement u_{10} in the midpoint of the follower link: H_c ranging from 1 to 55. H_p=35 and T_s=1 ms.

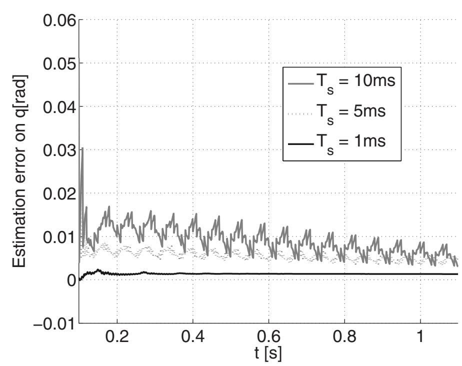

Fig. 8 Elastic displacement u_{10}: estimation error with T_s ranging from 1 ms to 10 ms. H_p=35 and H_c=10.

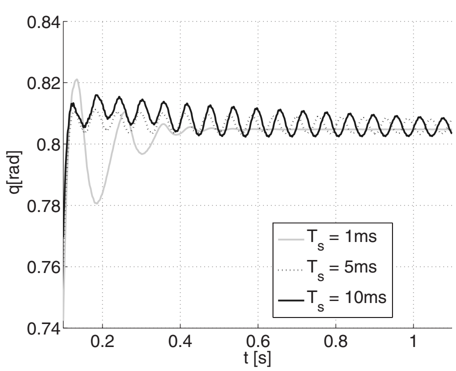

Fig. 6 Angular position of the crank q: T_s ranging from 1 ms to 10 ms. H_p=35 and H_c=10.

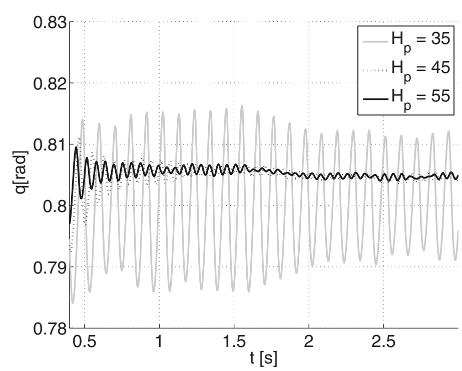

Fig. 9 Non-nominal plant. Angular position of the crank q: H_c ranging from 35 to 55. H_p=10 and T_s=1 ms.

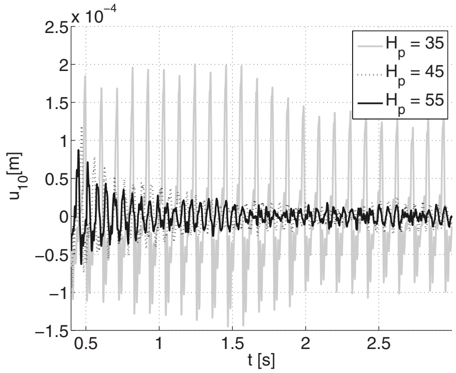

Fig. 10 Non-nominal plant. Elastic displacement u_{10}: H_c ranging from 35 to 55. H_p=10 and T_s=1 ms.

prediction horizon H_p. This is a well known result [10]. Therefore, for the mechanism discussed in this work, a suitable trade-off between robustness and hardware computation constraints can be obtained by assuming the following MPC values: H_c=10, H_c =45, and T_s=1 ms.

4 Conclusions

A high accuracy FEM-based dynamical model of a four-bar flexible link mechanism is presented in this paper. This model has been employed in a software simulation environment to investigate the effectiveness of the MPC control strategy for vibration damping in flexible closed-loop planar mechanisms. In order to implement the control system, a linearized model of the dynamic system has been developed. The effects of using different choices for the MPC parameters have been investigated. The robustness of the proposed control system has been numerically proven as well. The MPC control appears to be very effective both for reference position tracking and vibration suppression.

Nomenclature

q = angular position of the crank
$\mathbf{u}$ = vector of nodal displacements of the ERLS
u_i = ith nodal displacement
$\mathbf{x}$ = state vector
$\mathbf{M}$ = mass matrix
$\mathbf{K}$ = stiffness matrix
$\mathbf{S}$ = sensitivity matrix
$\mathbf{I}$ = identity matrix
$\mathbf{g}$ = vector of gravity accelerations
$\mathbf{f}$ = vector of the external forces acting on the nodes
$\mathbf{M}_G$ = matrix of Coriolis acceleration contributions
α, β = Rayleigh damping constants
E = Young's modulus
J = flexural inertia moment
a = width of the link
b = thickness of the link
m = mass/unit of length of link
L_i = length of the ith link
k = discrete time variable
$w(k)$ = control variable
$\mathbf{z}(k)$ = vector of controlled variables
$\hat{x}(k|t)$ = estimated value of the generic variable x for the time k obtained from values available at time t
$\mathbf{X}^T$ = transpose of the generic matrix $\mathbf{X}$
$\mathbf{r}(k)$ = vector of reference values
T_s = sampling time of the MPC controller
H_p = prediction horizon of the MPC controller
H_c = control horizon of the MPC controller
μ_9, μ_{10}, and μ_q = weights on u_9, u_{10}, and u_q, respectively

References

[1] Dwivedy, S. K., and Eberhard, P., 2006, "Dynamic Analysis of Flexible Manipulators, A Literature Review," Mech. Mach. Theory, **41**, pp. 749–777.
[2] Nagarajan, S., and Turcic, D. A., 1990, "Lagrangian Formulation of the Equations of Motion for Elastic Mechanisms With Mutual Dependence Between Rigid Body and Elastic Motions: Part II—Systems Equations," ASME J. Dyn. Syst., Meas., Control, **112**, pp. 215–224.
[3] Giovagnoni, M., 1994, "A Numerical and Experimental Analysis of a Chain of Flexible Bodies," ASME J. Dyn. Syst., Meas., Control, **116**, pp. 73–80.
[4] Boscariol, P., Gasparetto, A., and Zanotto, V., 2009, "Vibration Reduction in a Single-Link Flexible Mechanism Through the Synthesis of an MPC Controller," *Proceedings of the IEEE International Conference on Mechatronics*, Malaga, Spain, Apr. 14–17.
[5] Hassan, M., Dubay, R., Li, C., and Wang, R., 2007, "Active Vibration Control of a Flexible One-Link Manipulator Using a Multivariable Predictive Controller," Mechatronics, **17**, pp. 311–323.
[6] Gasparetto, A., and Zanotto, V., 2006, "Vibration Reduction in a Flexible-Link Mechanism Through Synthesis of an Optimal Controller," Meccanica, **41**, pp. 611–622.
[7] Trevisani, A., 2003, "Feedback Control of Flexible Four-Bar Linkages: A Numerical and Experimental Investigation," J. Sound Vib., **268**, pp. 947–970.
[8] Caracciolo, R., and Trevisani, A., 2001, "Simultaneous Rigid-Body Motion and Vibration Control of a Flexible Four-Bar Linkage," Mech. Mach. Theory, **36**(2), pp. 221–243.
[9] Gasparetto, A., 2001, "Accurate Modeling of a Flexible-Link Planar Mechanism by Means of a Linearized Model in the State-Space Form for Design of a Vibration Control," J. Sound Vib., **240**(2), pp. 241–262.
[10] Maciejowski, J. M., 2002, *Predictive Control With Constraints*, Prentice Hall, Englewood Cliffs, NJ.